8. T. L. Johnson, L. J. Olsen, *Plant Physiol.* **127**, 731 (2001).
9. A ~700-bp Sal I–Pst I GFP fragment and a ~1.1-kb Kpn I–Sal I *TED3* cDNA fragment (EST F6H9T7, ABRC, Ohio State University) were cloned into pCHF3 containing the 35S promoter (C. Fankhauser, J. Chory, unpublished data).
10. A Sac I–Sal I *TED3* cDNA fragment was cloned into pCHF3.
11. A ~700-bp Sal I–Bam HI fragment containing the promoter and the first 43 nucleotides of the coding sequence of *TED3* was cloned into the *GUS* gene fusion plasmid pBI101.3 (Clontech, Palo Alto, CA).
12. J. Hu, J. Chory, unpublished data.
13. M. Hayashi, K. Toriyama, M. Kondo, M. Nishimura, *Plant Cell* **10**, 183 (1998).
14. B. K. Zolman, I. D. Silva, B. Bartel, *Plant Physiol.* **127**, 1266 (2001).
15. Cotyledons grown for 5 days in light were fixed for 21 hours at 4°C with 2.5% glutaraldehyde, 2% paraformaldehyde, and 3.75% acrolein in phosphate buffer and were processed as described by H-m. Li, K. Culligan, R.A. Dixon, and J. Chory [*Plant Cell* **7**, 1599 (1995)].
16. A ~1.1-kb Kpn I–Sal I *TED3* cDNA fragment was cloned into pCHF3.
17. Chip experiment was conducted using 5-day dark- or light-grown seedlings according to the instructions from Affymetrix (Santa Clara, CA). Cluster analysis was performed using GeneSpring 4.1.1 (Silicon Genetics, Redwood City, CA).
18. D. Schroeder *et al.*, *Curr. Biol.*, in press.
19. F. J. Corpas, J. B. Barroso, L. A. del Rio, *Trends Plant Sci.* **6**, 145 (2001).
20. P. Mullineaux, L. Ball, C. Escobar, B. Karpinska, G. Creissen, S. Karpinski, *Philos. Trans. R. Soc. London Ser. B* **355**, 1531 (2000).
21. E. Lopez-Huertas, W. Charlton, B. Johnson, I. Graham, A. Baker, *EMBO J.* **19**, 6770 (2000).
22. A. Konieczny, F. M. Ausubel, *Plant J.* **4**, 403 (1993).
23. K. Boudonck, L. Dolan, P. J. Shaw, *J. Cell Sci.* **111**, 3687 (1998).
24. We thank M. Chen, D. Schroeder, and Y. Zhao for comments on the manuscript; D. Trelease for the catalase and pAPX antiserum; J. Harada for the ICL and MS antiserum; and B. Bartel and X. W. Deng for the *pxa1* and *cop1* seeds. Supported by a National Science Foundation grant to J.C. and the Howard Hughes Medical Institute.

Supporting Online Material
www.sciencemag.org/cgi/content/full/297/5580/405/DC1
Table S1

6 May 2002; accepted 17 June 2002

Integrin-Mediated Long-Term B Cell Retention in the Splenic Marginal Zone

Theresa T. Lu and Jason G. Cyster*

The mechanisms that control localization of marginal zone (MZ) B cells are poorly understood. Here we show that MZ B cells express elevated levels of the integrins LFA-1 (αLβ2) and α4β1 and that they bind to the ligands ICAM-1 and VCAM-1. These ligands are expressed within the MZ in a lymphotoxin-dependent manner. Combined inhibition of LFA-1 and α4β1 causes a rapid and selective release of B cells from the MZ. Furthermore, lipopolysaccharide-triggered MZ B cell relocalization involves down-regulation of integrin-mediated adhesion. These studies identify key requirements for MZ B cell localization and establish a role for integrins in peripheral lymphoid tissue compartmentalization.

Most blood that enters the spleen is released into the marginal sinus; from there, it flows through the macrophage- and B cell–rich MZ, before it returns to the circulation through venous sinuses (*1*, *2*). This enormous flow of blood ensures that B cells situated in the MZ, which includes the bulk of splenic B cells in humans (*3*), readily come in contact with systemic antigens. B cell entry into the MZ compartment is regulated by B cell receptor signaling (*4*, *5*), and the compartment is enriched for immunoglobulin M–positive (IgM^+) memory B cells (*6*) and cells that react with bacterial antigens (*7*) and autoantigens (*8*–*10*). The sessile, nonrecirculatory state of MZ B cells (*3*) contrasts with the migratory state of follicular B cells and suggests that the mechanisms that control their localization are likely to be distinct. Consistent with this, the chemokine/receptor pair CXCL13 (BLC)/CXCR5, which is critical for B cell migration to lymphoid follicles (*11*) and to the body cavities (*12*), is not needed for B cell lodgment within the MZ. Therefore, we considered whether B cells may lodge in the MZ in response to other factors and investigated the contribution of adhesion molecules. Measurement of surface integrin levels on MZ B cells, which account for about 5% of spleen B cells in C57BL/6 mice, revealed elevated expression of αL and β2 integrin subunits on MZ B cells compared with follicular B cells. Thus, MZ B cells have higher amounts of the αLβ2 heterodimer LFA-1 (Fig. 1A). MZ B cells also expressed greater amounts of β1-containing integrins than follicular B cells, but they had equal levels of α4-containing and lower levels of β7-containing integrins (Fig. 1A). Staining with an antibody specific for α4β7 revealed lower expression of this heterodimer on MZ B cells (Fig. 1A). Although antibodies specific for murine α4β1 are not available, the only known partners for α4 are β1 and β7. Therefore, we conclude that MZ B cells express higher levels of α4β1 than follicular B cells.

We next tested the functional status of LFA-1 and α4β1 on MZ and follicular B cells with an ex vivo adhesion assay (*13*). MZ B cells bound substantially better than follicular B cells to the LFA-1 ligand ICAM-1 and to the α4β1 ligand VCAM-1 (Fig. 1B). Adhesion to ICAM-1 could be inhibited by a blocking antibody to αL, which confirms the role of LFA-1 and rules out contributions by other β2 integrins (Fig. 1B). Similarly, adhesion to VCAM-1 could be inhibited with an antibody to α4 (Fig. 1B). Although α4β7 can also function as a receptor for VCAM-1, an α4β7-neutralizing antibody did not block adhesion of MZ B cells to VCAM-1 (*14*). The MZ is located adjacent to the CXCL13-rich follicle and, after being released in the MZ, recirculating follicular B cells migrate to the follicle in response to CXCL13 (*11*). Therefore, we examined how the relative differences between follicular and MZ B cell integrin activity influenced CXCL13-mediated chemotaxis. MZ and follicular B cells showed similar dose sensitivities for CXCL13 (Fig. 1C), although the maximal MZ B cell response was typically lower than the response of follicular cells. When we compared the chemotactic response of cells on uncoated and on VCAM-1–coated Transwell filters, MZ B cell migration was strongly retarded in the presence of VCAM-1, whereas follicular B cell migration was enhanced (Fig. 1C). Previous studies in other systems have shown that optimal integrin-ligand densities enhance cell motility, but, at densities above a critical threshold, migration is retarded (*15*). Our findings indicate that, at ligand densities that augment follicular B cell migration, the high levels of functional integrins on MZ B cells are sufficient to prevent cells from migrating to CXCL13.

We next examined the functional relevance of LFA-1 and α4β1 to MZ B cell localization in vivo. Three hours after we treated mice with a combination of α4 and αL blocking antibodies, MZ B cell numbers in the spleen were reduced and large numbers of MZ phenotype B cells were present in the blood (Fig. 2, A and B). This effect was specific for MZ B cells, because follicular B cell numbers in the spleen showed no change

Howard Hughes Medical Institute, Department of Microbiology and Immunology, and Division of Pediatric Immunology and Rheumatology, University of California, 513 Parnassus Avenue, San Francisco, CA 94143, USA.

*To whom correspondence should be addressed. E-mail: cyster@itsa.ucsf.edu

after antibody treatment (*14*). Although follicular B cell numbers were increased in the blood, this was associated with the expected block in B cell entry to lymph nodes (*16*). Immunohistochemical analysis of spleen tissue from mice 3 hours after antibody treatment revealed complete displacement of B cells from the MZ, whereas the follicles and T zones remained grossly intact (Fig. 2C). In contrast to the striking effect on MZ B cells, the treatment did not affect distribution of MZ macrophages (*13*, *14*). Complete displacement of MZ B cells from the MZ (Fig. 2C) but only partial displacement from the spleen (Fig. 2B) most likely results from their presence in splenic blood. Treatment with either α4 or αL blocking antibody alone caused the displacement of small numbers of MZ B cells (Fig. 2B). Analysis of mice 4 days after combined treatment with antibodies to α4 and αL revealed that MZ B cells had

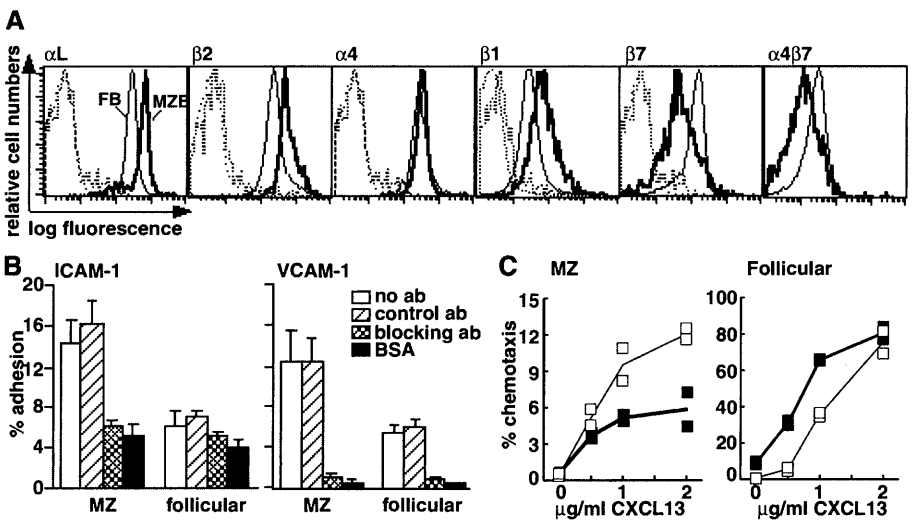

Fig. 1. Elevated integrin expression and adhesion of MZ B cells. (**A**) Flow cytometric analysis of integrin levels on B220^{+}CD23$^{lo/-}$CD21^{hi} MZ B cells (MZB; thick solid line) and B220^{+}CD23^{hi}CD21^{+} follicular B cells (FB; thin solid line). Dashed lines are staining controls for MZ (thick dash) and follicular (thin dash) B cells. β2$^{-/-}$ splenocytes were used as a control for β2 staining, and staining without primary antibody was used for the other integrin subunits. Mean fluorescence intensity d. from several experiments are shown in table ›1. (**B**) Integrin-mediated adhesion to ICAM-1 and VCAM-1. Splenocytes were allowed to adhere to plastic coated with ICAM-1 (10 μg/ml) or VCAM-1 (3 μg/ml) and adherent subsets were enumerated by flow cytometry (*13*). Blocking antibody on ICAM-1 was the αL antibody, and on VCAM-1 it was the α4 antibody, both at 500 ng/ml. Control antibodies were isotype matched to the blocking antibody. Background adhesion is measured by adhesion on bovine serum albumin (BSA) in the absence of ligand. Bars represent the mean of triplicate determinations (±SD) and data are representative of at least three experiments. (**C**) MZ B cell chemotaxis to CXCL13 (BLC) in the presence or absence of integrin ligand. Spleen cells were placed in Transwell chambers coated (*13*) with either BSA (open symbol, thin line) or VCAM-1 (filled symbol, thick line) and allowed to migrate toward the indicated concentrations of CXCL13. Assays were done in duplicate, and the lines connect mean values at each concentration tested. Data are representative of at least three experiments.

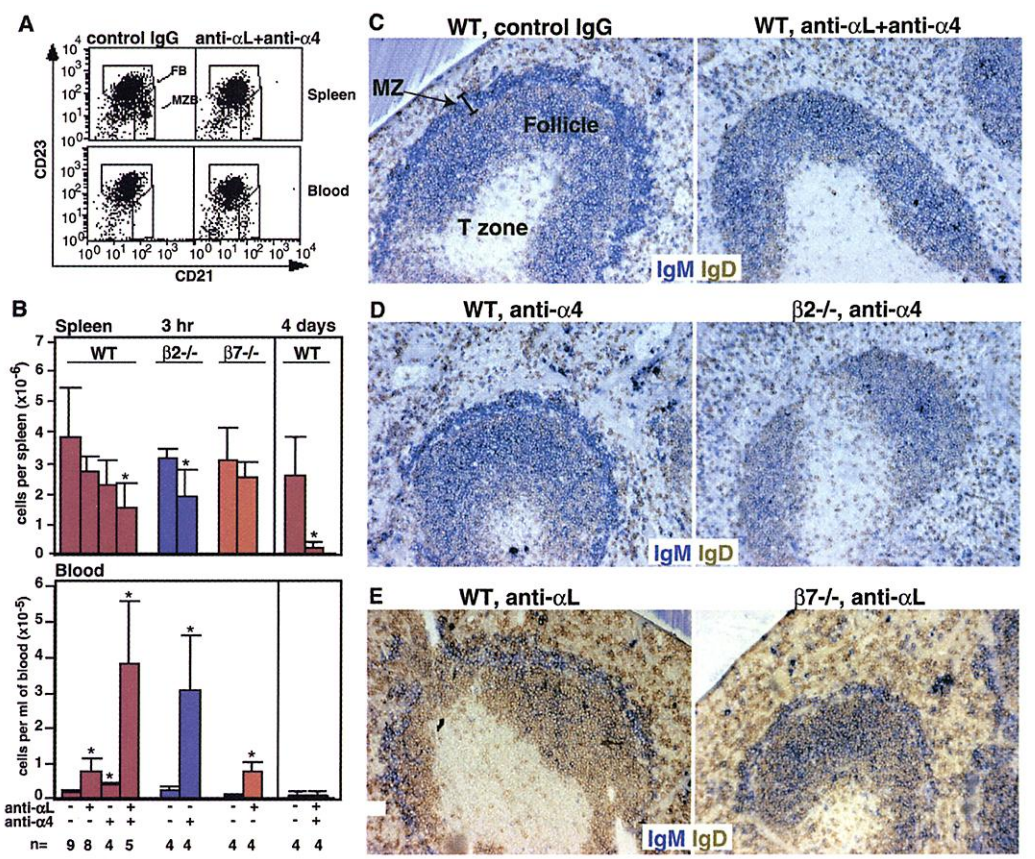

Fig. 2. Displacement of MZ B cells by combined inhibition of LFA-1 and α4β1. (**A**) Flow cytometric analysis of spleen and blood from mice treated for 3 hours with 100 μg each of α4 and αL antibodies or isotype-matched control antibodies. (**B**) Number of B220^{+}CD23$^{lo/-}$CD21^{hi} MZ B cells in spleen (upper) and blood (lower) after antibody treatment. Wild-type, β2$^{-/-}$, and β7$^{-/-}$ mice were treated for 3 hours with the indicated antibody combinations and cell populations were enumerated by flow cytometry. Wild-type mice were also analyzed 4 days after antibody injection. Bars represent the mean (±SD) values for data from the indicated number of mice per group. Effects of antibody treatment are compared with the control antibody-treated group; *, $P < 0.05$ by unpaired Student's *t* test. (**C**) Immunohistochemical analysis of spleen sections from wild-type mice treated with isotype control or αL and α4 antibodies for 3 hours and stained for IgM (blue) and IgD (brown). MZ B cells (IgM^{hi}/IgD^{lo}) normally surround the IgM^{lo}/IgD^{hi} B cell follicles, which surround the central T cell zone (*1*). Sections are representative of at least four mice for each condition. Objective magnification, ×10. (**D**) Spleen sections from wild-type and β2$^{-/-}$ mice treated for 3 hours with α4 antibody. (**E**) Spleen sections from wild-type and β7$^{-/-}$ mice treated for 3 hours with αL antibody. Sections from β2$^{-/-}$ and β7$^{-/-}$ mice treated with control antibody are shown in fig. S1.

been lost from both spleen and blood (Fig. 2B).

Spleens from $\beta2^{-/-}$ mice (*17*) and from wild-type controls contained similar frequencies of MZ B cells (Fig. 2B; fig. S1A), but treatment with α4 blocking antibody was sufficient to fully displace the MZ B cell population, in contrast to the limited effect of this single antibody treatment in wild-type mice (Fig. 2, B and D). Analysis of $\beta7^{-/-}$ mice that lack the α4β7 and αEβ7 integrins (*18*) revealed normal numbers of MZ B cells and treatment of these animals with αL blocking antibody led to minimal release of MZ B cells (Fig. 2, B and E; fig. S1B). This effect was similar to that observed in controls treated with antibody to αL (Fig. 2, B and E) and excluded a requirement for β7-containing integrins. These observations indicate that LFA-1 and α4β1 make substantial and mostly overlapping contributions to B cell retention within the MZ.

Immunohistochemical analysis of spleen tissue for ICAM-1 and VCAM-1 (*13*) showed that these molecules are strongly expressed in the MZ (Fig. 3, A and B). Notably, the intensity of ICAM-1 staining in the MZ was greater than in other areas of the spleen (Fig. 3A). Although strong VCAM-1 staining was also evident in the red pulp, expression within the MZ corresponded to a broad zone, whereas red-pulp staining was punctate and associated with individual cells (Fig. 3B). Analysis of ICAM-1–deficient mice (*19*) revealed normal numbers of MZ B cells, but treatment with antibody to α4 was sufficient to completely displace the cells from the MZ (Fig. 3, C to E). Therefore, ICAM-1, and not ICAM-2 or ICAM-3, functions as the relevant LFA-1 ligand in MZ B cell localization. When we reconstituted lethally irradiated ICAM-1–deficient mice with wild-type bone marrow, ICAM-1 expression in the MZ was minimally restored and treatment with α4-blocking antibody was sufficient to cause displacement of most MZ B cells (Fig. 3C). Similar treatment of reciprocal chimeras (ICAM-1–deficient bone marrow into wild-type mice) was not sufficient to displace the MZ B cell population (Fig. 3C), which indicates that radiation-resistant cells make a dominant contribution to the ICAM-1 expression necessary for MZ B cell retention. Treating wild-type mice with a combination of antibodies to VCAM-1 and to αL (Fig. 3, C and F), or treating $ICAM\text{-}1^{-/-}$ mice with antibody to VCAM-1 alone (fig. S1C), was also sufficient to mediate complete displacement of MZ B cells, which indicates that VCAM-1 serves as the MZ ligand for α4β1.

The cytokine lymphotoxin (LT)α1β2 plays a critical role in the development of secondary lymphoid tissues, acting to transmit signals from hematopoietic cells to supportive stromal cells that promote chemokine and adhesion molecule expression (*20*). Although B cell production is not LTα1β2 dependent, development of the MZ B cell compartment requires this cytokine (*21*, *22*). The finding that ICAM-1 and VCAM-1 are critical components of the MZ B cell niche led us to ask whether the lack of MZ B cells in LTα1β2-deficient mice reflected a role for this cytokine in promoting MZ adhesion molecule expression. We treated adult mice with the LTα1β2 antagonist LTβ receptor-immunoglobulin (LTβR-Ig), for 2 weeks, a period that is sufficient to disrupt splenic follicular dendritic cell function (*23*). After this treatment, MZ B cell numbers were reduced by 60% (fig. S2) and MZ ICAM-1 levels were markedly diminished (Fig. 3, G and H). VCAM-1 expression in the MZ was also reduced, whereas expression in the red pulp appeared to be unaffected (Fig. 3, I and J). Taken together with the detection of LTβR expression on cells in the MZ (*24*), it appears likely that LTα1β2 directly induces ICAM-1 and VCAM-1 expression on MZ stromal cells and that this is a requirement for the maintenance of MZ B cells.

Although MZ B cells do not recirculate, they undergo rapid migration to lymphoid follicles after exposure to bacterial products, such as lipopolysaccharide (LPS), helping to transport systemic antigens to follicular dendritic cells (*1*, *3*, *7*). To test whether this relocalization (Fig. 4A) was associated with a LPS-triggered decrease in MZ B cell integrin activity, we carried out ex vivo adhesion assays. Within 3 hours of LPS exposure, MZ B cells had undergone a decrease in adhesiveness to VCAM-1 and this decrease was more significant for both ligands after 6 hours (Fig. 4B). In chemotaxis assays with CXCL13, LPS-exposed MZ B cells were less strongly retained by VCAM-1, whereas they were unchanged in their chemotactic response in the absence of adhesion molecules (Fig. 4C). Treating CXCL13-deficient mice with LPS caused minimal MZ B cell redistribution in 3 hours but led to a partial displacement of cells

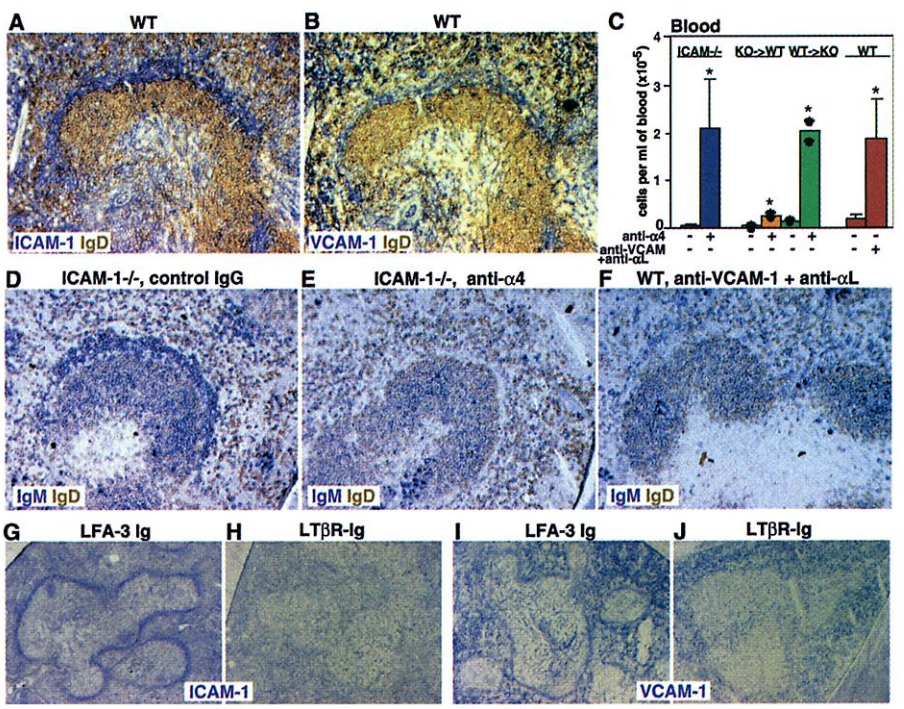

Fig. 3. Expression patterns of ICAM-1 and VCAM-1 and their role in MZ B cell retention. (**A** and **B**) Immunohistochemical detection of ICAM-1 or VCAM-1 (blue) and IgD (brown) in sections of spleen from wild-type mice treated for 3 hours with αL and α4 antibodies (*13*). (**C**) MZ B cell numbers in blood of $ICAM\text{-}1^{-/-}$ mice treated with α4 antibody, $ICAM\text{-}1^{-/-}$ bone marrow chimeras (*13*) treated with α4 antibody, and wild-type mice treated with αL and VCAM-1 antibodies. KO→WT, wild-type recipients reconstituted with $ICAM\text{-}1^{-/-}$ bone marrow; WT→KO, $ICAM\text{-}1^{-/-}$ recipients reconstituted with wild-type bone marrow. Bars are mean (±SD) number obtained from at least four mice per group for the $ICAM\text{-}1^{-/-}$ and wild-type mice. Bone marrow chimera values were from two mice per group and each filled symbol represents one mouse. *, $P < 0.05$ by Student's *t* test. (**D** to **F**) Spleen sections from the indicated mice that had been treated for 3 hours as indicated, stained to detect IgM (blue) and IgD (brown). Objective magnification, ×10. (**G** to **J**) Requirement for LTα1β2 in maintenance of marginal zone ICAM-1 and VCAM-1 expression. Immunohistochemical detection of ICAM-1 and VCAM-1 in spleens of control (LFA3-Ig)- or LTβR-Ig–treated mice, as indicated, that had each been given αL and α4 antibodies 3 hours before analysis (*13*). Objective magnification, ×5.

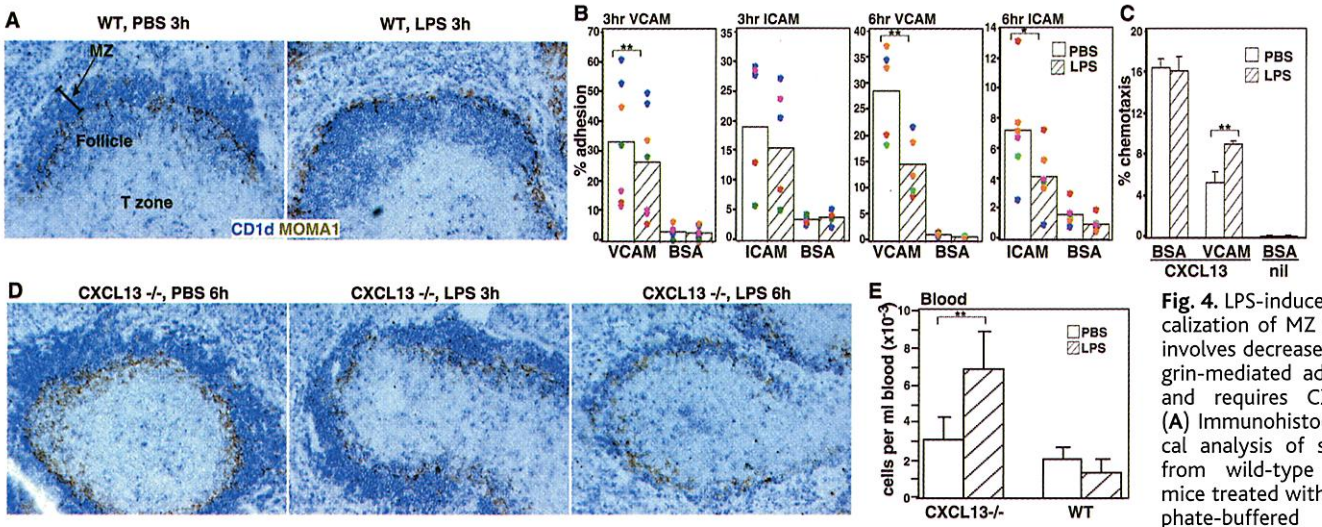

Fig. 4. LPS-induced relocalization of MZ B cells involves decreased integrin-mediated adhesion and requires CXCL13. (**A**) Immunohistochemical analysis of spleens from wild-type (WT) mice treated with phosphate-buffered saline (PBS) or LPS for 3 hours. Splenic sections were stained to detect CD1d^{hi} MZ B cells (blue) and MOMA-1–positive marginal metallophilic macrophages (brown) (*13*). Location of CD1d^{hi} MZ B cells relative to CD1d$^{lo/-}$ follicles in the control spleen section is indicated. Objective magnification, ×10. (**B**) Adhesion on VCAM-1 (3 μg/ml) or ICAM-1 (6 to 10 μg/ml) coated plastic of MZ B cells from mice treated with PBS or LPS for 3 or 6 hours (*13*). Each filled symbol represents data from one mouse, and symbols of the same color within one graph represent paired mice from the same experiment. Bars represent mean values obtained from the pooled data. (**C**) MZ B cell chemotaxis to CXCL13 or no chemokine (nil) across BSA- or VCAM-1–coated membranes of Transwell chemotaxis chambers. Cells were from mice treated for 3 hours with PBS or LPS. MZ B cells were identified as B220^{+}CD23$^{lo/-}$CD1d^{hi}. Data shown are representative of more than 10 experiments. Migration in the absence of chemokine was similar on BSA- and VCAM-1–coated filters (*14*). (**D**) Immunohistochemical analysis of spleens from CXCL13-deficient mice treated with PBS or LPS for 3 or 6 hours. Sections were stained as in (A). (**E**) MZ B cell numbers in the blood of CXCL13$^{-/-}$ or control wild-type mice treated with LPS for 6 hours. MZ B cells were identified as in (C). *, $P < 0.05$; **, $P < 0.01$ in paired (B) or unpaired [(C) and (E)] Student's t test.

from the MZ after 6 hours (Fig. 4D). Flow cytometric analysis revealed that significant numbers of MZ B cells were released into the blood of CXCL13$^{-/-}$ but not wild-type mice after 6 hours of LPS exposure (Fig. 4E). Only small numbers of MZ B cells moved into white-pulp areas in treated CXCL13$^{-/-}$ mice, perhaps migrating in response to the T cell zone chemokines CCL19 (ELC) and CCL21 (SLC). These observations indicate that in vivo exposure to LPS induces a decrease in integrin adhesive function in MZ B cells. We propose that decreased adhesiveness, together with other undefined changes, allows MZ B cells to migrate to follicles in response to CXCL13.

The findings described above establish that LFA-1 and α4β1 participate in controlling cell compartmentalization in a peripheral lymphoid tissue, extending their previously established roles in cell trafficking across endothelium (*16*, *25*, *26*) and in cell retention within the bone marrow (*27*). We propose that, during their development, MZ B cells up-regulate levels of functional LFA-1 and α4β1, and when they are released into the MZ they are captured and retained by the ICAM-1 and VCAM-1 expressed by resident stromal cells. While such a mechanism may obviate the need for chemokine-mediated guidance to the MZ, the involvement of chemotactic factors is not excluded. The discovery that MZ B cell retention is integrin-mediated agrees well with the finding that Pyk2-deficient mice lack MZ B cells (*28*), as Pyk2 is activated downstream of LFA-1 and α4β1 (*29*). Similarly, the requirement for the rac activator Dock2 for MZ B cell development or accumulation (*30*) may reflect a requirement for Dock family molecules in integrin signaling, and the requirement for Isc (also known as p115RhoGEF) (*31*) is consistent with the ability of Rho to mediate integrin activation. Our findings also suggest that accumulation of the MZ B cell population depends on LTα1β2-mediated development of an adhesive niche in the spleen. Displacing B cells from this niche by blocking integrin function might be a way to purge the compartment of autoreactive or malignant cells.

References and Notes

1. G. Kraal, *Int. Rev. Cytol.* **132**, 31 (1992).
2. E. E. Schmidt, I. C. MacDonald, A. C. Groom, *Scanning Microsc.* **7**, 613 (1993).
3. I. C. M. MacLennan, D. Gray, D. S. Kumararatne, H. Bazin, *Immunol. Today* **3**, 305 (1982).
4. A. Cariappa *et al.*, *Immunity* **14**, 603 (2001).
5. F. Martin, J. F. Kearney, *Curr. Opin. Immunol.* **13**, 195 (2001).
6. D. K. Dunn-Walters, P. G. Isaacson, J. Spencer, *J. Exp. Med.* **182**, 559 (1995).
7. F. Martin, J. F. Kearney, *Immunol. Rev.* **175**, 70 (2000).
8. C. M. Grimaldi, D. J. Michael, B. Diamond, *J. Immunol.* **167**, 1886 (2001).
9. U. Wellmann, A. Werner, T. H. Winkler, *Eur. J. Immunol.* **31**, 2800 (2001).
10. Y. Li, H. Li, M. Weigert, *J. Exp. Med.* **195**, 181 (2002).
11. K. M. Ansel *et al.*, *Nature* **406**, 309 (2000).
12. K. M. Ansel, R. B. Harris, J. G. Cyster, *Immunity* **16**, 67 (2002).
13. Materials and methods are available as supporting material on *Science* Online.
14. T. T. Lu, J. G. Cyster, unpublished observations.
15. D. M. Rose, V. Grabovsky, R. Alon, M. H. Ginsberg, *J. Immunol.* **167**, 2824 (2001).
16. C. Berlin-Rufenach *et al.*, *J. Exp. Med.* **189**, 1467 (1999).
17. K. Scharffetter-Kochanek *et al.*, *J. Exp. Med.* **188**, 119 (1998).
18. N. Wagner *et al.*, *Nature* **382**, 366 (1996).
19. H. Xu *et al.*, *J. Exp. Med.* **180**, 95 (1994).
20. Y.-X. Fu, D. D. Chaplin, *Annu. Rev. Immunol.* **17**, 399 (1999).
21. R. E. Mebius, S. van Tuijl, I. L. Weissman, T. D. Randall, *J. Immunol.* **161**, 3836 (1998).
22. R. Ettinger *et al.*, *J. Exp. Med.* **193**, 1333 (2001).
23. F. Mackay, G. R. Majeau, P. Lawton, P. S. Hochman, J. L. Browning, *Eur. J. Immunol.* **27**, 2033 (1997).
24. M. Murphy *et al.*, *Cell Death Differ.* **5**, 497 (1998).
25. E. C. Butcher, *Cell* **67**, 1033 (1991).
26. T. A. Springer, *Cell* **76**, 301 (1994).
27. T. Papayannopoulou *et al.*, *Blood* **97**, 1282 (2001).
28. R. Guinamard, M. Okigaki, J. Schlessinger, J. V. Ravetch, *Nature Immunol.* **1**, 31 (2000).
29. J. T. McDonald, R. M. Teague, S. H. Benedict, M. A. Chan, *Immunol. Invest.* **29**, 71 (2000).
30. Y. Fukui *et al.*, *Nature* **412**, 826 (2001).
31. I. Girkontaite *et al.*, *Nature Immunol.* **2**, 855 (2001).

32. We thank E. Ekland and T. Okada for help and reagents; J. Browning for LTβR-Ig; E. Brown for β2$^{-/-}$ mice; E. Brown, S. Luther, M. Matloubian, and T. Okada for comments on the manuscript; and E. von Scheven for help with statistical analysis. T.T.L. is a National Institute of Child Health and Human Development (NICHD) Fellow of the Pediatric Scientist Development Program (NICHD grant award K12-HD00850) and J.G.C. is a Packard Fellow. Supported by the Howard Hughes Medical Institute and by National Institutes of Health grant AI-40098.

Supporting Online Material

www.sciencemag.org/cgi/content/full/297/5580/409/DC1

Materials and Methods

Figs. S1 and S2

Table S1

7 March 2002; accepted 17 June 2002